Blowing jets as a circulation flow control to enhancement the lift of wing or generated power of wind turbine

Alexandru DUMITRACHE*,[1], Florin FRUNZULICA[1,2], Horia DUMITRESCU[1], Vladimir CARDOS[1]

*Corresponding author
*,[1]"Gheorghe Mihoc-Caius Iacob" Institute of Mathematical Statistics and Applied Mathematics of the Romanian Academy
Calea 13 Septembrie no. 13, 050711 Bucharest, Romania
alex_dumitrache@yahoo.com*, horiadumitrescu@yahoo.com, v_cardos@yahoo.ca
[2]"POLITEHNICA" University of Bucharest, Faculty of Aerospace Engineering,
Polizu no.1-6, RO-011061, Bucharest, Romania
ffrunzi@yahoo.com

DOI: 10.13111/2066-8201.2014.6.2.4

Abstract: *The goal of this paper is to provide a numerical flow analysis based on RANS equations in two directions: the study of augmented high-lift system for a cross-section airfoil of a wing up to transonic regime and the circulation control implemented by tangentially blowing jet over a highly curved surface due to Coanda effect on a rotor blade for a wind turbine. This study were analyzed the performance, sensitivities and limitations of the circulation control method based on blowing jet for a fixed wing as well as for a rotating wing. Directions of future research are identified and discussed.*

Key Words: *numerical flow analysis, high-lift system, blowing jet, trailing edge blowing*

1. INTRODUCTION

It is well-known that obtaining high lift coefficients especially in certain phases of flight (take-off, landing) is very important in the field of aircraft. But a high lift coefficient is desirable to be also obtained to other devices that run on an air stream, such as, for example, turbo machines, the wind turbines being a particular case. There are two different methods to achieve this goal: the first one that implies changing of the airfoil shape and the second method that does not require changing of the airfoil geometry of the wing or blade. These conventional high-lift systems imply the existence of slats or slotted flaps, running on trailing-edge or leading-edge of wing. Some of the main disadvantages of the conventional augmenting lift systems are: mechanical complexity, and noise pollution, especially around airports or in the vicinity of the wind farm turbines.

With the development of technology these disadvantages have been reduced. In the last years alternative methods have been used and studied as a new class of innovative transport systems capable to reduce noise around airports at an admissible level of current standards. These are the so-called gapless high-lift systems, capable to replace the systems based complex mechanisms [1]. In this work a high-lift configuration like an airfoil is investigated which utilises trailing edge blowing, as an active flow control. One wing with such a circulation control (CC) is capable to generate the required lift coefficients for the take-off or landing flight segment, even if it uses a fraction of at most 5% of the cold engine flow. Since

the absence of slots allows obtaining laminar flows on the wing in the cruise flight, the drag will be reduced, which means less fuel consumption.

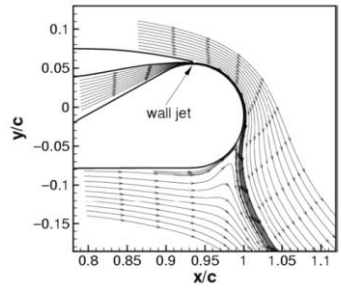

Figure 1: Typical circulation control on airfoil near the trailing edge

A graph showing the trailing edge of the airfoil configuration is shown in Fig. 1. The wall jet emanating from the plenum "sticks" to the trailing edge surface due to the Coanda effect [2], causing delayed flow separation and thus increasing circulation and producing higher lift. The second flow analysis is used to investigate the aerodynamic performance of a wind turbine rotor equipped with circulation control technology (blowing jet). The highly beneficial impact to lift-to-drag ratio from using the Coanda jet can be seen in Ref. [3] and provided the motivation for investigating technology in the present study.

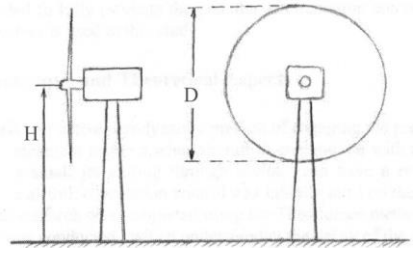

Figure 2: Sketch of Horizontal Axis Wind Turbine (HAWT)

In practice, the rotor axis of a wind turbine rotor is usually not aligned with the wind because the wind keeps changing its direction continuously. If the blades are connected to a vertical shaft, the turbine is called a vertical axis wind turbine (VAWT), and if the shaft is horizontal, the turbine is called a horizontal axis wind turbine (HAWT). Most commercial wind turbines are the HAWTs. A HAWT is described in terms of the rotor diameter (D), the number of blades, the tower height (H), the rated power (P) and the control system. The rated power is the maximum power allowed for the installed generator, and the control system must ensure that this power is not exceeded in high winds. The number of blades is often two or three. The aerodynamic efficiency is lower on a two-bladed than on a three-bladed wind turbines. A high rotational speed of the rotor is desirable in order to reduce the gearbox ratio required and this leads to low solidity rotors. In the yawed flow condition, the induced velocity varies both azimuthally and radially which makes the aerodynamics of the wind turbine even more complicated for yawed flow than for axial flow conditions. Under certain conditions, blade-vortex interactions can occur. These factors may lead to flow separation, inflow gradient across the rotor disk, and dynamic stall. The principal effects of separation on aerodynamic characteristics summarized as follows:

- Increased drag (wide wake)
- Increased instability (formation of free shear layer)
- Loss of lift

The category of the separated-flow control is related to the flow that has fully separated (as angle of attack increases beyond stall, fully separated flow develops and becomes a bluff -body type flow).

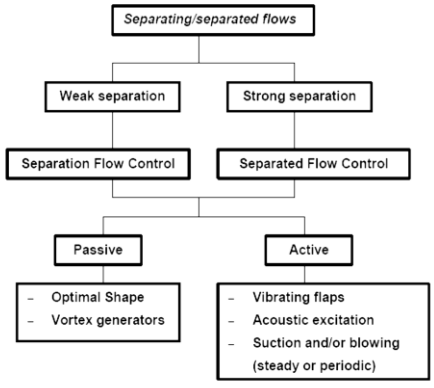

Figure 3: Possible flow control strategies

Attempts at modelling these effects have been limited due to the computational complexity. Main active control techniques are boundary layer suction to remove the low momentum fluid, wall heat transfer to control and modify the viscosity of the fluid and momentum addition to the boundary layer by steady and unsteady blowing. Circulation control is implemented by tangentially blowing a small high-velocity jet over a highly curved surface, such as a rounded trailing edge (Fig. 1). This causes the boundary layer and the jet sheet to remain attached along the curved surface due to the Coanda effect (a balance of the pressure and centrifugal forces) and causing the jet to turn without separation.

A systematic study is thus needed to fully evaluate the benefits of circulation control technology for wing or wind turbine rotor/blade. A viscous solver is used in this study.

2. CIRCULATION CONTROL TECHNIQUE AND THEORETICAL ASPECTS

Circulation control (CC), a passive or active aerodynamic method of changing the properties (lift, camber or angle of attack) has been used as an enhancement to fixed wing aircraft in conjunction with a Coanda surface [4-7]. Just from the beginning it must be shown that a small jet exiting through a slot can have a relatively large influence on the aerodynamic characteristics of an airfoil. The circulation control was initially used on the cylinder and then applied to an elliptical airfoil. In 1975, further research was completed using the Theodorsen method in a potential flow analysis [8]. Later, a Coanda simulation was conducted which under predicted the decay of the maximum jet velocity [9].

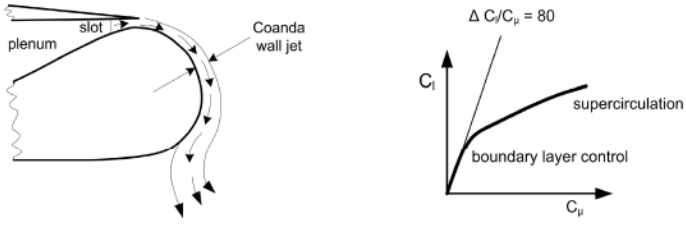

a) Rounded trailing edge b) Schematic lift behaviour

Figure 4: Basic of circulation control flow

The jet sheet remains attached along the curved surface due to the Coanda effect. The rear stagnation point location moves toward the lower airfoil surface, producing additional increase in circulation around the entire airfoil. The outer irrotational flow is also substantially turned, leading to high value of lift coefficient comparable to that achievable from conventional high lift systems, as indicated in Fig. 4(b). In the 1970's the circulation control research passed to the optimization of the parameters: slot placement, the height of the slot, favourable momentum coefficient, the pressure into plenum. The expansion of CC was used to submarine and rotary wing. During the 1990's-2000's the CC techniques became more predictable and the research includes the capability to reduce the amount of additional hardware to the original systems. They are already used to several previously non-investigated variants, including several vehicles - not only aircraft - such as tractor trailers, cars, wind turbines and water turbines. In the last years numerical flow simulations capability offers new opportunities to the development of efficient lift augmentation systems, like a blown flaps. The current numerical approach is mainly based on the Reynolds - averaged Navier-Stokes (RANS) equations. Several models of turbulence were studied and evaluated. Computations using RANS without a suitable turbulence model to take into account the curvature effect, would fail to predict separation and the lift accurate. When using a flow control facility providing mass addition in the system (for example, the jet blowing), mathematically, this involves introducing an additional circulation term taking into account the jet reaction forces:

$$P = \rho V_{\infty} \left(\Gamma_c + \Gamma_{jet} \right) \tag{1}$$

where Γ_c is circulation (around the body),

$$\Gamma_{jet} = \frac{\dot{m} V_{jet}}{\rho V_{\infty}} \left(\alpha + \beta_{jet} \right) \tag{2}$$

and $\dot{m}$ is the mass flow rate of the jet with the speed V_{∞}, while β_{jet} is the jet orientation (relative to airfoil chord). The following aerodynamic coefficients result:

$$\begin{aligned} C_{L,jet} &= C_T \sin\left(\alpha + \beta_{jet} \right) \\ C_{D,jet} &= C_T \cos\left(\alpha + \beta_{jet} \right) \end{aligned} \tag{3}$$

where C_T is the thrust coefficient generated by the jet. The term provided by the counteracting force might affect the lift and drag and depends on the angle between the jet ejection direction and the airfoil chord (Fig. 5).

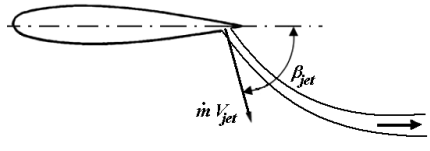

Figure 5: Thrust force due to a fluid flap (fixed jet position)

The efficiency of a fluid flap (a jet normally oriented to the surface) compared to the efficiency of circulation control airfoils (a tangential jet on the upper side of the airfoil) depends on the difference between the induced effects that accompany the pressure fields. It's known that both techniques applied for an airfoil take benefit from the induced and counteracting forces, strongly depending on the airfoil jet's position [10,11]. The fluid flap airfoil is strongly dependent on the counteracting force of the jet momentum. The

Circulation control systems on "Coanda" surfaces "capture" the induced forces more efficiently and, generally, generate a higher lift than a fluid flap airfoil. For the circulation control systems, the jet orientation is rear, determining a counteracting force with a restricted contribution to lift (except the cases when the airfoil curvature leads to a β_{jet} angle) (Fig. 6). The jet in the vecinity of a "Coanda" surface modifies the induced (two-dimensional) circulation.

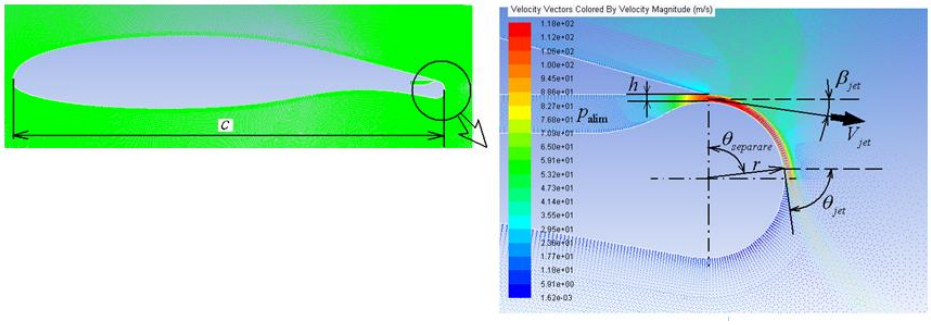

Figure 6: Scheme of geometric elements associated to the "Coanda" type flow

It's recognized that the efficiency of a rectangular nozzle depends on the geometry of its section (dimension's ratio in the section plane). The efficiency studies for rectangular nozzles are limited to the aspect ratio of 10 (Aspect Ratio = *w/h*) while for similar studies used in circulation control this ratio is higher than 1300, thus the provided results cannot be extrapolated to determine the recovered thrust. Therefore, for the two-dimensional study presented, the efficiency of the nozzle might be neglected and it can be presumed that there are no (pressure) losses; whereas for the circulation control two-dimensional study the thrust might be assessed at the airfoil exit of the blown jet using the momentum coefficient:

$$C_{\mu} = \frac{Thrust}{qS} = \frac{\dot{m}V_{jet}}{qS} = \frac{2hw}{bc}\frac{\rho_{jet}}{\rho_{\infty}}\frac{V_{jet}^2}{V_{\infty}^2} \tag{4}$$

where

$$\dot{m} = \rho_{jet} V_{jet} h w \tag{5}$$

and *S* is the wing reference surface (considered as rectangular), while

$$V_{jet} = \sqrt{\frac{2\chi RT_{0,jet}}{\chi - 1}\left[1 - \left(\frac{p_{\infty}}{p_{0,jet}}\right)^{\frac{\chi-1}{\chi}}\right]} \tag{6}$$

Optimizing the engine thrust in the case of circulation control involves specifying geometry details of the airfoil, the geometry of the intake system, pipes, a compressor and an outlet. If these details are missing, the control system's benefits and failures are performed by estimating the necessary power for flow circulation control. For a rough estimation of the fluid's power, P_f, it is presumed that the jet is supplied by a big reservoir. Then, the total power will be at least equal to the power required to supply the control device to create the jet (P_{jet}) plus the lost power in the intake device of the big reservoir (P_{rez}):

$$P_f = P_{jet} + P_{rez} = \frac{1}{2}\rho V_{jet}^2 \frac{\dot{m}}{\rho} + \dot{m}V_{\infty}^2 \tag{7}$$

Also, the necessary power to be supplied for the flow with the momentum coefficient C_{μ} is:

$$P_f = C_\mu \frac{V_{jet}}{2V_\infty}\left[1+2\frac{V_\infty^2}{V_{jet}^2}\right](q_\infty V_\infty S) \tag{8}$$

or dimensionless

$$C_{P_f} = \frac{P_f}{q_\infty V_\infty S} = C_\mu \frac{V_{jet}}{2V_\infty} + C_\mu \frac{V_\infty}{V_{jet}} \tag{9}$$

If the nozzle height *h* is constant and known for a rectangular wing, the fluid power might be expressed as a function of the momentum coefficient C_μ and the nozzle height /airfoil chord ratio (*h/c*):

$$C_{P_f} = \frac{C_\mu^{3/2}}{2\sqrt{2(h/c)}}\left[1+\frac{4(h/c)}{C_\mu}\right] \tag{10}$$

Figure 7 shows the dependence of the ideal power coeffcient as function of the momentum coefficient.

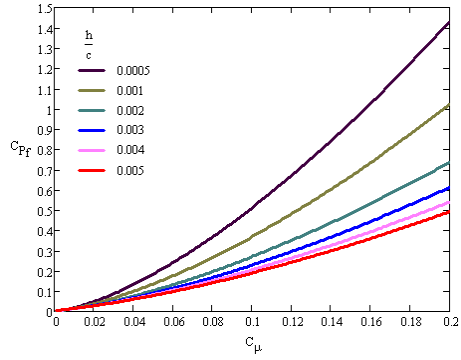

Figure 7: Necessary theoretic power for typical "Coanda" jets with different *h/c* ratio

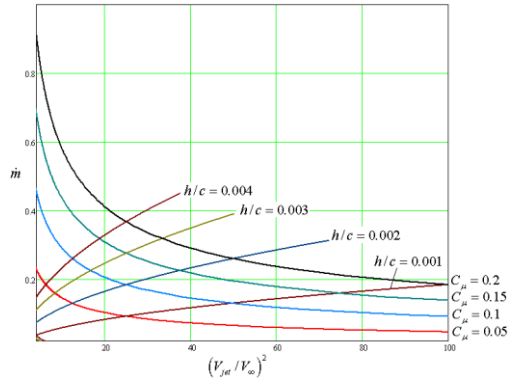

Figure 8: Necessary mass flow (ideally) for circulation control ($c = 0,5m; V_\infty = 30m/s; T_0 = 291K$)

To optimize the performances of the circulation control system for the lowest mass flow (jet), it is necessary to know the relation between the mass flow ($\dot{m}$), the momentum coefficient C_μ and the nozzle geometry. Figure 8 shows the dependency results for $\dot{m} = f(C_\mu, h/c)$ in fixed condition for external flow and a given geometry. Assuming that the system performance is practically provided by the velocities ratio V_{jet}/V_∞, reducing the nozzle height, a reduced mass flow will be necessary.

3. INVESTIGATION OF THE FLOW CONTROL USING THE COANDA EFFECT ON AN AIRFOIL

During the last decade, experiments, flight tests and, last but not least, numerical simulation and experiments have revealed the major benefits provided by flow control using the Coanda effect [10, 11, 12]. From those, we mention: reaching a high lift coefficient ($C_{Z,\max} \cong 3$); while the availability of slats/ flaps increases performances; flight evolution at high incidence; modifying the Coanda surface geometry according to the flight conditions leads to increased aerodynamic performance; minimizing drag by double blowing at trailing edge in cruising flight; stabilizing the aircraft during different lateral manoeuvring, etc.

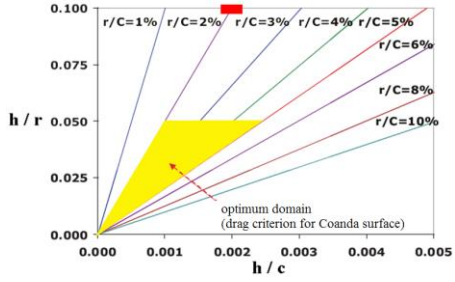

Figure 9: Effective performances for the "Coanda" effect in cruise flight (subsonic compressible regime)

Even if such benefits are available, these control techniques are not (yet) implemented in (mainly, civil) aircraft manufacturing because of several reasons, namely: a number of pipes/ channels are required to take-over the blowing flow from the engine; certain configurations require a special engine positioning; increases in drag during certain evolutions because of the thick trailing edge (which includes blowing elements and the "Coanda" control surface).

One of the main disadvantages is the control system maintenance, since a high efficiency requires relatively small-dimension slots, which can be easily obliterated. Probably, this generates high maintenance costs. The requirement for large radius Coanda surfaces for maximum lift is frequently replaced by minimum drag requirement in cruise flight, leading to small radius Coanda surfaces, as revealed by studies during the last decades [10, 11] (Figure 9). For our applications the configuration was selected for h/c = 0.002, h/r=0.1, while r/c = 2 % - the red rectangle in Figure 9 (the Coanda surface is a half circle, β_{jet} = 0^0). The numeric study was conducted on a supercritical profile with the relative thickness of 17%, having large radius joints at the leading edge to minimize the stall (separation) phenomenon. The reference airfoil is GAW(1), the modified one being NASA LaRC 2D 17% *Supercritical General Aviation Circulation Controlled Airfoil* (GACC) with a round trailing edge r/c=2% (the airfoil was generated based on available data existent in scientific literature) [11, 12]. The Reynolds number was set as Re=10^6 to provide a fully turbulent flow; airflow in the convergent device which generate jet was presumed to be turbulent. The momentum coefficient is determined from the equation (8), where q is the dynamic pressure for undisturbed flow (far away from airfoil) $q = \rho V_\infty^2 / 2$, and the reference surface is $S = b \cdot c = 1 \cdot c$. From the computational point of view, the mesh have a number of nodes of order 10^5; near to solid surfaces, a structured mesh is used, providing values between 0.4 and 1 for y^+ (the dimensionless distance from the wall), and between 25 and 300 for Δx^+. The computation domain has far field boundaries at around $20 \cdot c$ distance, the boundary conditions being typical for 2D aerodynamic analysis. The RANS model is solved with the "pressure-based" scheme, while the selected turbulence model was $k-\omega$ SST

(Shear Stress-Transport Turbulence Model) proposed by Menter [11], which included the surface curvature effect. The solver was unsteady, the time step being the physical one automatically assessed by the solver [12]. Two constructive solutions are analyzed based on the GACC airfoil: one with a cylindrical trailing edge surface (geometrical dimensions being previously defined), and a second configuration involving a blowing flap.

The results are shown for the 0^0 incidence and different momentum coefficients C_μ; while the undisturbed flow has a velocity $V_\infty = 30 m/s$.

3.1 Test case 1. Flap with cylindrical surface

The jet leaves the slot under $\beta_{jet} = 0^0$ angle and has the tendency to remain attached to the surface on a certain length. As shown from the representation of streamlines, a low momentum jet influenced by the external flow on the upper side of airfoil will be quickly separate, practically after some degrees, having a minor contribution to lift increase (the main jet component being thrust). The jet attachment depends on the jet momentum coefficient, the slot height, the Coanda surface geometry and, not least, on the external flow velocity (due to friction effects, the jet catches external flow fluid). Increasing the jet momentum, the separation angle will exceed 90^0 (the jet has a light reverse) and it would penetrate the low momentum flow on the lower side of the airfoil generating a "fluid slat" (or a virtual slat). It should be remarked that the jet has a positive influence on the outboard flow for moderate incidence limiting the boundary layer separation.

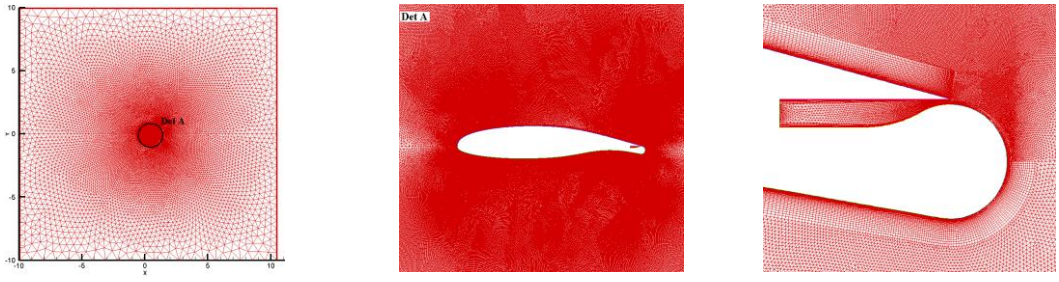

Figure 10: Computational domain and meshing details

A jet with high momentum coefficient, correlated with a very low *h*/*r* ratio leads to a compressible flow regime in the slot and its vicinity, therefore the use of a compressible solver being preferred, with all the numerical problems occurring from it.

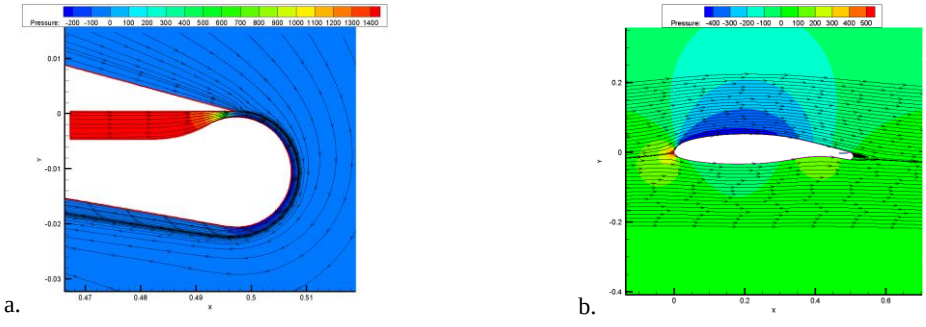

a. b.

Figure 11: Streamlines and pressures field: (a) without external flow ($V_{entr} = 9\ m/s,\ V_\infty = 0\ m/s$) and (b) external flow without jet ($V_\infty = 30\ m/s$)

The jet angle θ_{jet} is a characteristic of the Coanda effect, while a value higher than 90^0 ($x/c = 1$) generates the increasing of the suction pressure on the lower side of the Coanda

surface and reduces the surface lift efficiency rate. For input speeds, in the plenum chamber, higher than 9 m/s (average speed) the numerical result shows a complete jet attachment on the cylindrical trailing edge surface, with reverse on the lower side of the airfoil, also confirmed by experiences conducted on this airfoil [10, 11, 12] (Figure 11). In the figures 12-13 the streamlines and detail of the pressure field near to trailing edge can be seen, for different momentum coefficients (only extreme cases were shown).

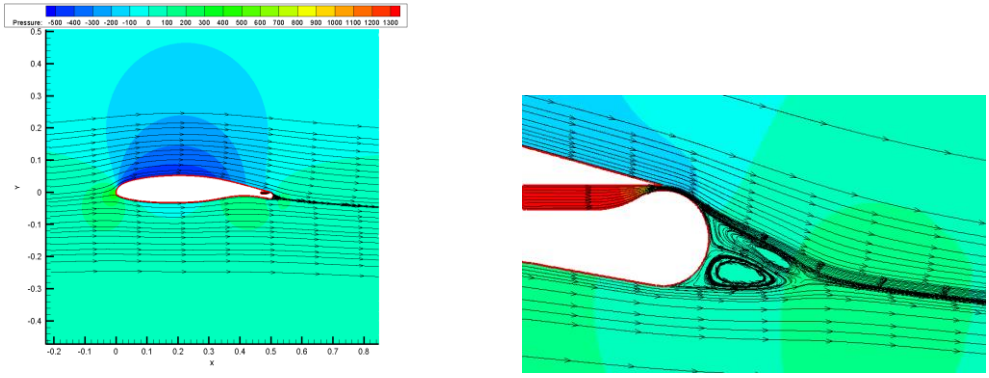

Figure 12: Streamlines and pressures field (TE details on the right): for $V_{entr} = 9\ m/s,\ V_{\infty} = 30\ m/s$

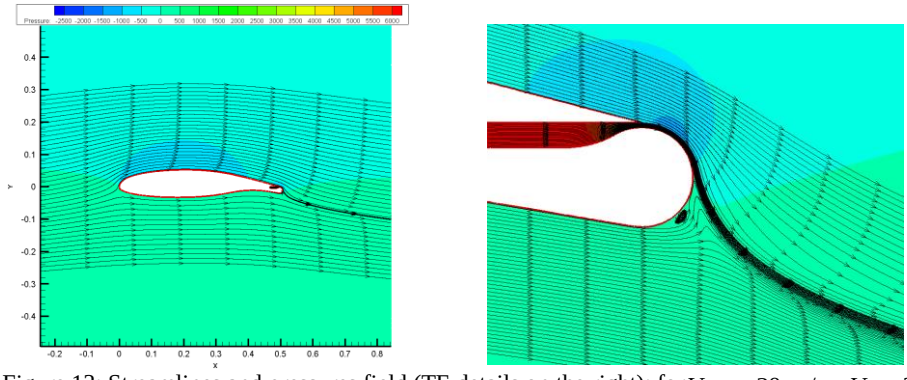

Figure 13: Streamlines and pressures field (TE details on the right): for $V_{entr} = 20\ m/s,\ V_{\infty} = 30\ m/s$

3.2 Test case 2. Flap with double curvature

The second numerical test replaces the trailing edge with cylindrical surface with a double-curvature flap (the flap has a cylindrical upper part with the same radius that in test case 1). The flap has a 55^0 deflection angle to enable the better assessment of blowing efficiency. Up to a reservoir entrance velocity of 10.549 m/s ($C_{\mu} = 0.0124$), the jet is relatively quickly separating in a domain of 10^0-20^0 (on the cylindrical surface).

The jet is fully reattaching to the flap surface if the supply velocity is higher than 10.55 m/s. The jet is separating effectively, from the flap trailing edge, while penetrating the flow on the lower side of the airfoil. The numerical results are presented in figures 14 and 15. As a conclusion regarding the first two tests, the blowing efficiency on a "Coanda" surface, compared with reference $(C_{\mu} = 0)$ is immediately observed. For the higher impulse the jet will remain attached on the "Coanda" surface, even with a flow reverse tendency.

Concerning the jet efficiency with a relatively high deflection flap (in our case 55^0), it will be noticed that for momentum coefficient higher than $C_{\mu} = 0.0123$, the jet is immediately reattached to the flap surface, increasing its

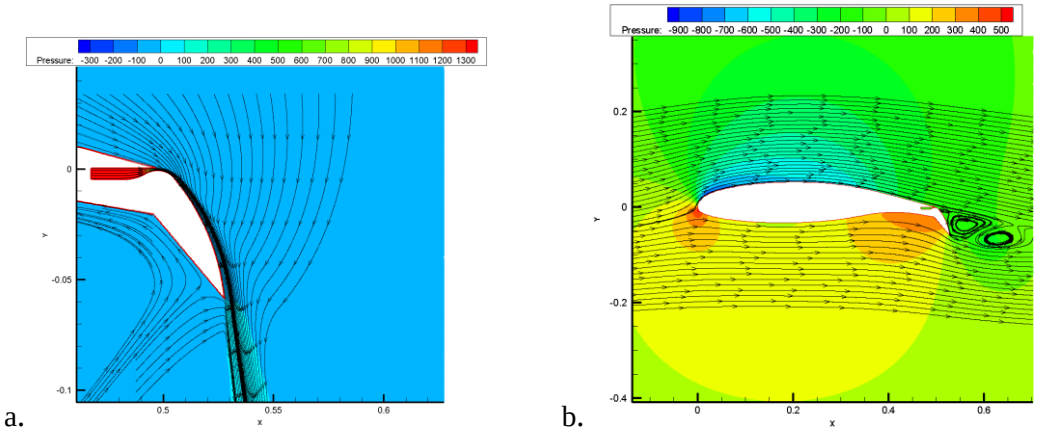

Figure 14: Streamlines and pressures field: (a) without external flow ($V_{entr} = 9\ m/s,\ V_\infty = 0\ m/s$) and (b) external flow without jet ($V_\infty = 30\ m/s$)

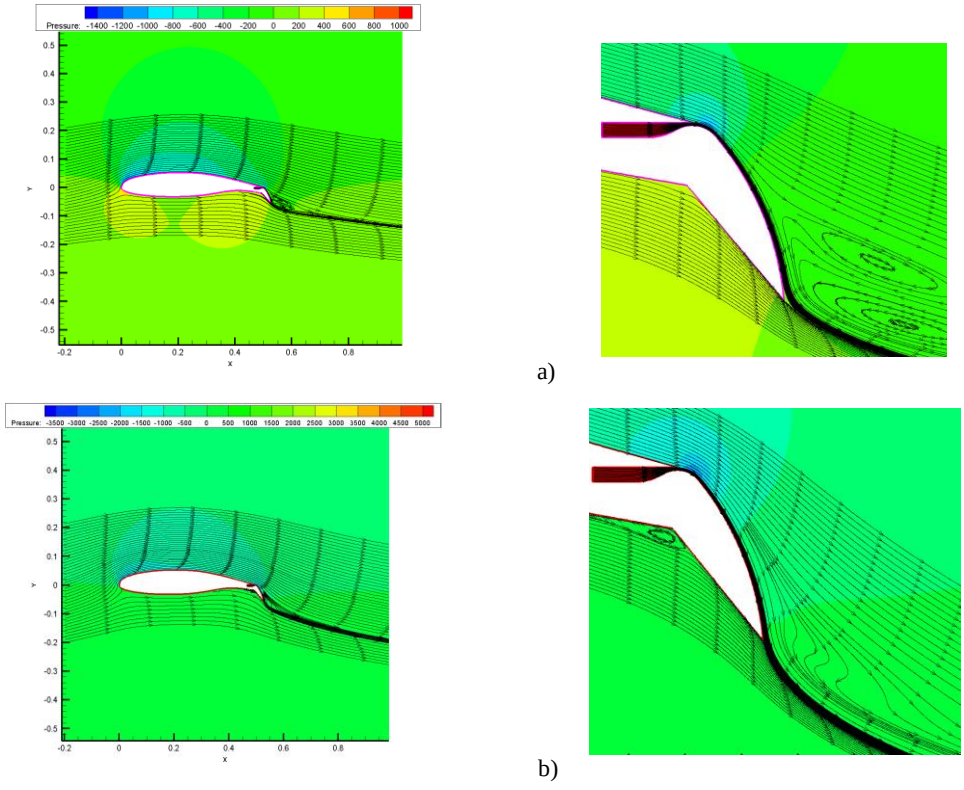

Figure 15: Streamlines and pressures field for two computation cases:
a) $V_{entr} = 10.55\ m/s,\ V_\infty = 30\ m/s$; b) $V_{entr} = 20\ m/s,\ V_\infty = 30\ m/s$

momentum coefficient higher than $C_\mu = 0.0123$, the jet is immediately reattached to the flap surface, increasing its efficiency, while the lift coefficient may increase to more than 200% of the reference value, but paying the cost of a drag increase.

It can be stated that thin jets in the proximity of a "Coanda" surface have a favourable impact on the aerodynamic characteristics, necessary during take-off / landing procedures, as well as in certain flight manoeuvres involving high load factors flight.

3.3 Test case 3. Cross-section of an aircraft wing with blown flap

The third case considered here refers to the cross section of an aircraft wing (for a medium-size transport aircraft**)** with a mean aerodynamic chord of $c = 6\ m$. The dimensionless slot height is h/c = 0.001 for this case. In the cross section the airfoil with a dual-radius flap is shown in Figure 16 [15].

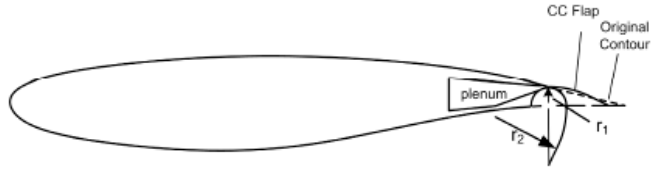

Figure: 16 A dual-radius circulation control airfoil [15]

A flap of about 10% chord radius pivots around a hinge. Because the upper surface of the flap has such a curvature that the Coanda effect can be exploited even at higher flow turning angles. There are three options to design the upper surface of the flap, Figure 17.

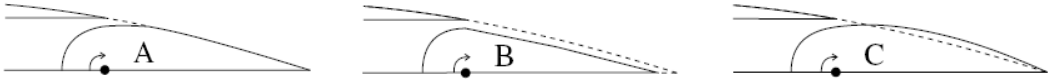

Figure 17: Geometric design version for the blown flap [15]

In the first version (A) the Coanda surface radius is hidden in the geometry of the airfoil during the cruise flight, but it appears if the flap is deflected for take-off or landing.

In the second version (B) the upper surface downstream of the flap is moved downwards by translation. Thus a small backward facing step is created, because in cruise flight, the upper surface of the flap is slightly below than the main airfoil.

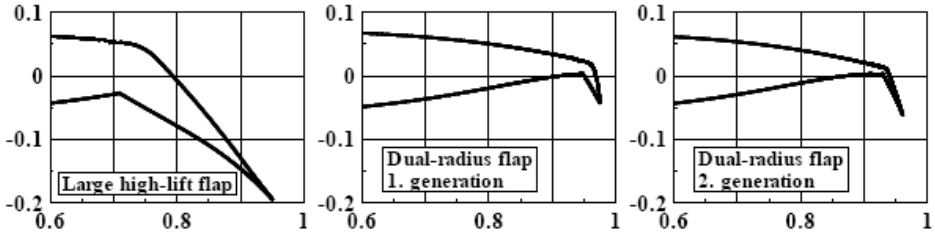

Figure 18: Possible flap geometries for airfoil with CC [16]

The last version (C) is a dual-radius flap, first time designed by Englar [16]. The second radius for the upper surface of the flap is used to obtain additional turning, then a higher lift. From this type a flaps a second generation was developed with a much better performance in cruise, at least for the transonic regime (Figure 18).

For a relative slot height of *h/c* = 0.001, a slot flow total pressure $p_{t,\,jet} / p_{\infty} \cong 1.7$ and the momentum coefficients $C_{\mu} = 0.04$**,** a comparison of lift coefficients is shown in Figure 19. The flow parameters for the reference transonic airfoil used in investigations, are: *a*) for the landing: $M_{l\infty} = \mathbf{0.2}$, $\mathrm{Re} = 2.9 \cdot 10^7$; *b*) for cruise: $M_{l\infty} = \mathbf{0.7}$, $\mathrm{Re} = 3.5 \cdot 10^7$.

It can be seen that for a flap deflection angles of 20^0 the large high-lift flap generates a high lift coefficient up to $c_{l,\max} = 3.2$ and certainly will increase if the angle of deflection will be greater. The slot height can be increased with a beneficial increased of the lift coefficient but there is an optimum height for which a smaller amount of bleed air is needed.

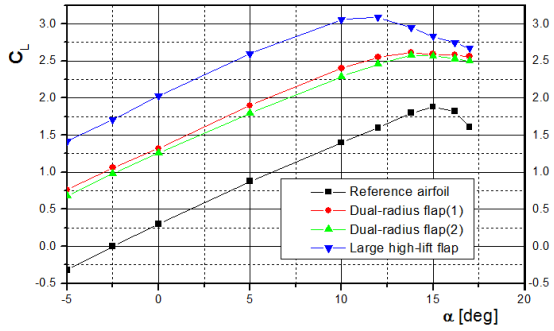

Figure 19: Variation $c_l(\alpha)$ for airfoil with different blown flap geometries. h/c = 0.0001
$M_{l\infty}$= **0. 2**, $Re = 2.9 \cdot 10^7$ **,** $c_\mu = 0.04$ **(** = 0.03 for the large high-lift flap)

It can be concluded that blowing decreases the angle of attack for which the maximum lift is produced. The data confirm the potential of blowing jet on a Coanda surface to generate high lift good for take-off or climb performance. Additional calculations are needed to optimize flap geometry and to determine the minimum total pressure and mass flow characteristics necessary to generate a certain lift, even for a 3D wings. Thus we obtain the needed parameters of blowing jet systems for a finite-span wing.

3.4. Blowing jet applied to the wind turbine blade

In the design of a new wind turbine today we have to use the latest aerospace engineering technology, including aerodynamics, lightweight materials (like a composite) and highly efficient aerodynamics (airfoils specially designed for the wind turbines, including circulation control technique) [23]. The concepts of circulation control through trailing edge blowing (Coanda jet) will be taken into account. The circulation control is implemented by tangential blowing a small high-velocity jet over a curved surface (Coanda surface), such as a rounded trailing edge (TE).

Computational modelling. Since a direct numerical simulation (DNS) of turbulent flow involving complex geometry such as HAWT is very costly, Reynolds-Averaged Navier-Stokes (RANS) are used in this study. It is necessary that the transition location to be specified. In our study, the Eppler's transition model is used [17]. An appropriate turbulence model will be the Spalart-Allmaras Detached Eddy Simulation (SA-DES) [18]. This is obtained from Spalart-Allmaras model by substituting the nearest distance to the wall *d*, everywhere in the transport equation, by the new DES length scale $\tilde{d}$, which is defined as $\tilde{d} = \min(d, C_{DES}\Delta)$. C_{DES} is an adjustable model constant, and Δ is based on the largest grid spacing in the *x*, *y*, or *z* directions forming the computation cell, $\Delta \equiv \max(\Delta x, \Delta y, \Delta z)$. After a proper calibration of the turbulence model, the constant values used in this work are specified [3]. The model constant C_{DES} = 0.65 was set in the homogeneous turbulence [19], and is also used in this study. The DES method attempts to combine the best aspects of RANS and LES in a single solution strategy. The law of the wall is characterized by a dimensionless distance from the wall defined as $y^+ = u_\tau y/\nu$, where u_τ is the friction velocity and ν is kinematic viscosity; y^+ is in the range $11 \le y^+ \le 300$. Because the governing equations are parabolic with respect to time and elliptic in space, initial and boundary conditions are required to solve these equations. In general, the initial flow conditions are set to free-stream values inside the flow field, which is enough to get the final convergence

solution with the time marching scheme. For instance, "non-slip" conditions are appropriate for the viscous surface, and "slip" conditions may be used in an "inviscid" simulation. For the CCW simulations, jet slot exit boundary condition must be specified to simulate the jet flow effects.

Jet Slot Exit. In most circulation control studies, the driving parameter of the jet is the momentum coefficient, C_μ, which is defined as follows:

$$C_\mu = \dot{m}V_{jet} \Big/ \left((1/2)\rho_\infty V_{ref}^2 A_{ref} \right) \tag{11}$$

where the jet mass flow rate is given by: $\dot{m} = \rho_{jet} V_{jet} A_{jet}$.

In the present study, the reference velocity V_{ref} is the rotor tip speed, and the reference area A_{ref} is the plan form area of the rotor blade. The total pressure and total temperature, T_0, of the jet are specified at the jet slot exit. These were estimated assuming a jet Mach number and isentropic relations. The jet is assumed to emanate in a direction tangential to the blade surface, and the pressure values at the jet are extrapolated from the pressure values in the outer flow over the airfoil. The jet velocity profile is specified to be parabolic at the jet exit. The effects of rotor tower and nacelle on the flow field have not been considered. All the calculations are done in a time-accurate manner. At low wind speeds 14,400 time steps are needed per blade revolution, representing the rotational movement of the blade by 1/40 deg. of azimuth every time step. At higher wind speeds, where unsteady effects are more dominant, a smaller time step equivalent to a 1/80 degree azimuth is used. The time step used in this study is in approximately $5\text{x}10^{-5}$ *s*, which is very small compared to the time constant for dynamic stall $\left(c/(\Omega r)\right)$ of NREL case which is approximately 0.01 *s*. Therefore, the time step chosen should be able to resolve dynamic stall.

3.5 Results and discussion

The validated flow solver is used to investigate the aerodynamic performance of a wind turbine rotor equipped with circulation control technology (blowing jet). The highly beneficial impact to lift-to-drag (L/D) ratio from using the Coanda jet can be seen in Ref. [20] and provided the motivation for investigating this technology in the study. Computational results are compared with the baseline rotor results to assess the benefits of the circulation control technology. Computations have been carried out at selected wind speeds representing both low and high wind speed regimes. The effects of the jet slot height or location on the performance of the Coanda jet have been investigated. For an effective Coanda-jet performance, a design of Coanda-configured TE has been chosen as in Figure 20. It was used an idea of a flat surface on lower surface near TE and a curved surface on the upper side [21]. Further investigations should be done to determine the proper TE radius and TE jet thickness which have a critical effect on the effectiveness of this blowing jet system.

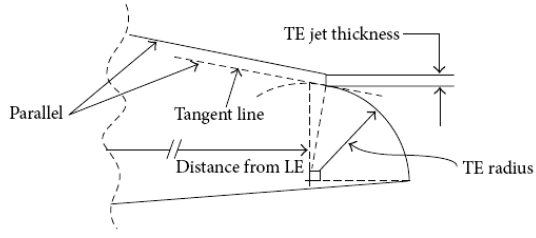

Figure 20: TE construction of the circulation control configured airfoil [22]

Computational Grid. The computational grid used for baseline rotor analysis is used here with a dense grid near the slot and in the vicinity of trailing edge. In this study, the jet slot is located at 93% of the chord on the upper surface of the rotor and the jet slot height is nominally 0.2% of the chord. In the present work, the jet slot runs along the entire span of the blade. The grid near the rotor surface and the jet slot is shown in Figure 21.

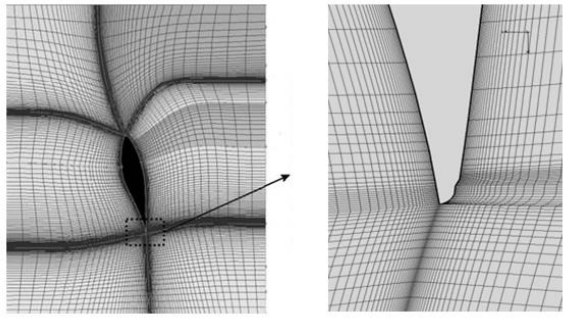

Figure 21: Computational grid around airfoil of CC rotor using for Coanda blowing jet (on the right side - detail of the mesh near the trailing edge of the blade)

The construction of a high quality grid around the circulation control airfoil is made difficult by the presence of a small jet slot. In the present study, an approach of treating the jet slot as a grid-aligned boundary is used as guidance, with the jet slot boundary condition described in previous section.

Test Conditions. Calculations have been obtained for the NREL Phase VI rotor at two wind speeds (7 and 15 m/s) and at three yaw angles (0, 10, and 30 degrees). The jet momentum coefficients C_μ used in this work range from 0 to 0.10. The reference values for these simulations are: freestream temperature T_∞ = 284 K, freestream density ρ_∞ = 1.225 kg/m^3 and reference chord length c = 0.483 m. The assessment of the present method was done by comparing the predictions with the following measurements: radial variation of the normal force coefficient C_N and tangential force coefficient C_T with varying of momentum coefficient, C_μ. Also investigations were performed concerning the effect of slot location on the L / D ratio and lift augmentation.

3.6 Circulation Control Results

Low Wind Speed Conditions. Only results at a low wind speed of 7 m/s for yaw angles up to 30 degrees are presented here. A visualization of the computed flow indicates that the flow is well-behaved and attached over much of the rotor. Therefore, on the present grid and the selected turbulence model, one can expect the results for the baseline case to be in reasonable agreement with measurements. Due to the Coanda effect, the jet remains attached to the curved trailing edge and provides enhanced suction on the trailing edge upper surface. In this work, the jet leaves the surface from a sharp trailing edge which fixes the rear stagnation point. As C_μ increases the front stagnation point moves backward on the lower surface, and there is a significant turning of the potential flow (outside of the boundary layer) over the airfoil causing an increase in circulation around the rotor section. The net turbine power output was calculated by accounting for the pumping power required to drive the slot blowing system. Figure 22 shows the radial distribution of the pressure normal and tangential force coefficients to the chord with varying C_μ. A reasonable agreement between prediction and measurements of the baseline case is observed for the no-blowing case at all

the yaw angles. As expected, the normal forces for the circulation control case are higher relative to the baseline no-blowing case. It is also seen that C_N increases as C_μ increases. At this low wind speed condition where the flow is well-behaved and attached over much of the rotor, the lift force is increased and also turned forward as a result of the increased angle of attack. It is clearly seen that C_T (associated with the induced thrust component of lift) is increased when circulation control is used.

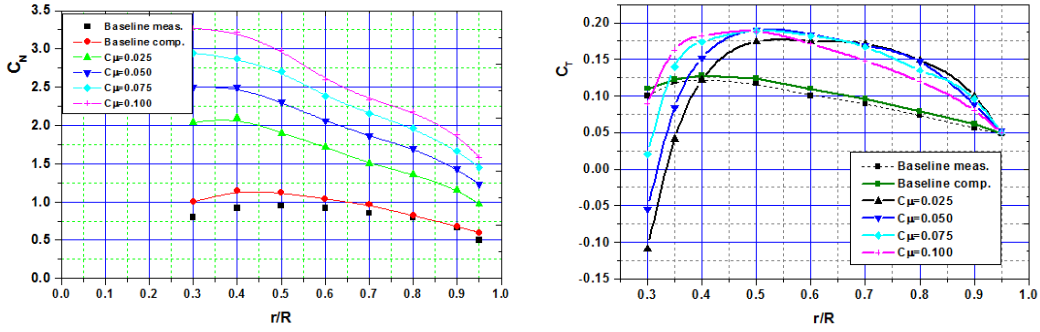

Figure 22: Radial distribution of the normal and tangential force coefficients C_N, C_T, at 7 m/s with varying C_μ

The circulation control technology requires power input into the system to generate the jets. The net power is the mechanical (shaft) power extracted from the wind minus the power input into the system to generate the jets. There should be a net positive increase in power generated for this concept to be attractive. The consumed power to generate the jet is proportional to the mass flow rate through the jet ($\rho_{jet} A_{jet} V_{jet}$) and the kinetic energy per unit mass of the jet ($(1/2)V_{jet}^2$). Thus, the power consumed in production of the jet is $(1/2)\rho_{jet} A_{jet} V_{jet}^3 / \eta_{sys}$, where η_{sys} is a parameter that takes into account losses or efficiencies associated with various components. Figure 24 shows the net excess power defined in percentage of baseline power. It is clearly seen that approximately up to C_μ = 0.070 there is net excess power production and the excess power production is clearly attributable to the circulation control technology. No net benefit was found at the higher C_μ values.

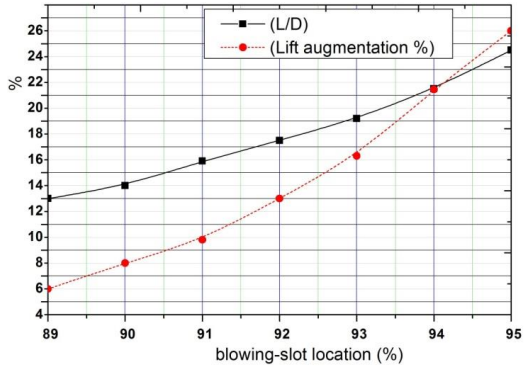

Figure 23: The effect of Coanda-jet location on the L/D ratio and lift augmentation

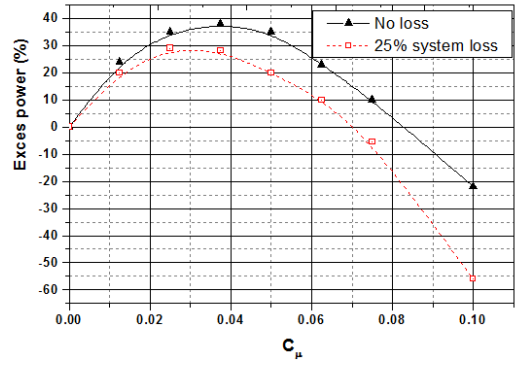

Figure 24: Net excess power vs. C_μ at 7 m/s (0° yaw)

Figure 23 shows the effect of slot location (in percent of chord) on the L / D ratio and lift augmentation. To identify an optimal configuration of the Coanda blowing-jet system, more detailed parametric study will be required including the effect of Coanda jet thickness,

the effect of TE radius or the effect of momentum coefficient on the L/D ratio and lift augmentation, i.e., overall, on the power generated by wind turbine equipped with such a system (beyond the scope of this study).

High Wind Speed Conditions. A second case studied is for a 15 m/s wind, where the wind speed is high enough to cause flow separation over the entire upper surface (not shown here). At 15 m/s the flow is fully separated over the rotor, and the Coanda jet is not as effective at generating lift as at the 7 m/s case. In this case, it has been found that there is a small change in lift; however, the drag is noticeably increased due to the enlarged effective area of wake over the rotor. It is seen that the outer flow is not affected by the trailing edge jet as much as it was at the low wind speed (7 m/s) case. No net power benefit was found at this high wind speed case.

4. CONCLUSION

Steady-state investigations on the high-lift configuration with Coanda-jet based on RANS solver are conducted. It was found that the use of this type of circulation control produces an equal or greater lift coefficients that those generated by conventional high-lift systems. The studies carried out thus far have shown that the effect of Coanda-jet is effective in producing enhanced lift.

Because these simulations are encouraging, additional calculations are needed to define the optimum flap geometry and to determine the optimum flow parameters linked to Coanda-jet system, needed to obtain the required lift. By physical reasoning and extension to three-dimensional case, enhanced sectional lift could then contribute to increased torque for the wind turbine applications. The following conclusion may be drawn from the study for the wind turbine blade:

- the present methodology is accurate for a range of wind speeds and yaw of interest to wind energy industry.At extreme wind conditions and yaw angles the method breaks down;
- for attached flow conditions, the circulation control technology (using trailing edge blowing and Coanda effect) is very effective at increasing the circulation around the airfoil section leading to a net increase in generated power as compared to the baseline rotor;
- at high wind speed conditions where the flow is separated, the trailing edge blowing becomes ineffective in increasing the power output.

Thus in this study the performance, sensitivities and limitations of the circulation control method were analysed based on blowing jet for a cross-section airfoil of a fixed wing as well as for a rotary wing.

Obviously, this method should be supplemented, where appropriate, with other methods of circulation control.

The present results are encouraging and can be further pursued for extended parametric studies and design oriented applications.

ACKNOWLEDGMENTS

This work was realized through the Partnership programme in priority domains - PN II, developed with support from ANCS CNDI - UEFISCDI, project no. PN-II-PT-PCCA-2011-3.2-1670 and was presented to the 2nd International Workshop on Numerical Modelling in Aerospace Sciences, NMAS 2014, 07 - 08 May 2014, Bucharest, Romania.

REFERENCES

[1] K. Pfingsten and, C. Radespiel, *Use of upper surface blowing and circulation control for gapless high lift configurations*, CEAS/ KATnet Conference on Key Aerodynamic Technologies. Bremen, Germany, 2005.

[2] Y. G. Zhulev and S. I. Inshakov, On the possibility of enhancing the efficiency of tangential blowing of a slit jet from an airfoil surface. *Fluid Dynamics*, **31**: 631-634, 1996.

[3] Y. Liu, L. N. Sankar, R. J. Englar, K. K. Ahujaand , R. Gaeta, *Computational Evaluation of the Steady and Pulsed Jet Effects on the Performance of a Circulation Control Wing Section*, AIAA Paper 2004-0056, 2004.

[4] C. E. Lan and J. F. Campbell, *Theoretical Aerodynamics of Upper-Surface Blowing Jet-Wing Interaction*, NASA TN D-7936, 1975.

[5] R. J. Englar, M. J. Smith, S. M. Kelley and R. C Rover, Application of Circulation Control to Advanced Subsonic Transport Aircraft, Part I: Airfoil Development. *Journal of Aircraft.* **31**: 1160-1168, 1994.

[6] R. J. Englar, M. J. Smith, S. M. Kelley and R. C. Rover, Application of Circulation Control to Advanced Subsonic Transport Aircraft, Part II: Transport Applications. *Journal of Aircraft.* **31**: 1169-1177, 1994.

[7] Y. Liu, *Numerical simulations of the aerodynamic characteristics of circulation control wing sections*, Ph.D. Thesis, Georgia Institute of Technology, 2003.

[8] E. H. Gibbs, *Analysis of Circulation Controlled Airfoils*. Ph.D. Thesis, West Virginia University, Morgantown, WV, 1975.

[9] R. A. Churchill, *Coandă Effect Jet Around a Cylinder with an Interacting Adjacent Surface*, Ph.D. Thesis. West Virginia University, Morgantown, WV.

[10] G. S. Jones, Pneumatic Flap Performance for a Two-Dimensional Circulation Control Airfoil In: *Applications of Circulation Control Technologies – Progress in Astronautics and Aeronautics*, **214**: 191-244, 2006.

[11] W. J. Baker and E.G. Paterson, Simulation of Steady Circulation Control for the General Aviation Circulation (GACC) Wing., In: *Applications of Circulation Control Technologies – Progress in Astronautics and Aeronautics.* **214**: 513–537, 2006.

[12] R. J. Englar, Overview of Circulation Control Pneumatic Aerodynamics: Blown Force and Moment Augmentation and Modification as Applied Primarly to Fixed-Wing Aircraft., In: *Applications of Circulation Control Technologies – Progress in Astronautics and Aeronautics.* **214**, 2006.

[13] F. R. Menter, Eddy viscosity transport equations and their relation to the k-ε model. *ASME Journal of Fluids Engineering*, **119**: 876-884, 1997.

[14] ***, Ansys Fluent 13.0. User's Guide.

[15] R. J. Englar and G. G. Huson, Development of Advanced Circulation Control Using High-Lift Airfoils. *Journal of Aircraft*. **21**: 476–483, 1984.

[16] R. J. Englar and R. A. Hemmerly, Design of the circulation control wing STOL demonstrator aircraft. *Journal of Aircraft*. **18** :51-58, 1981.

[17] G. Xu and L. N. Sankar, *Effects of Transition, Turbulence and Yaw on the Performance of Horizontal Axis Wind Turbines*, AIAA Paper 2000-0048, 2000.

[18] P. R. Spalart, W.-H. Jou, M. Strelets and S. R. Allmaras, *Comments on the Feasibility of LES for Wings and on a Hybrid RANS/LES Approach*, In: Proceeding of the 1st AFOSR International Conference on DNS/LES. Ruston, LA. 137-147, 1997.

[19] P. R. Spalart and S. R. Allmaras, *A One-Equation Turbulence Model for Aerodynamic Flows*. AIAA Paper 92-0439, 1992.

[20] S. Benjanirat, L. N. Sankar and G. Xu, *Evaluation of Turbulence Models for the Prediction of Wind Turbine Aerodynamics*, AIAA Paper 2003-0517, 2003.

[21] C. Tongchitpakdee, S. Benjanirat and L. N. Sankar, Numerical studies of the effects of active and passive circulation enhancement concepts on wind turbine performance. *J. of Solar Energy Eng.* **128**: 432–444, 2006.

[22] H. Djojodihardjo, M. F. Abdul Hamid, S. Basri, F. I. Romli and D. L. A. Abdul Majid. Numerical simulation and analysis of Coandă effect circulation control for wind-turbine application considerations. *IIUM Engineering Journal*. **12**: 19-42, 2011.

[23] Al. Dumitrache, F. Frunzulica, H. Dumitrescu and R. Mahu, Active and passive circulation control as enhancement techniques of wind turbines performance, *AIP Conference Proceedings*. 1493:330-334, 2012.